Study of ferromagnetic–spin glass threshold in $R_2Mo_2O_7$ by high-pressure neutron diffraction and μSR

2007 J. Phys.: Condens. Matter 19 145214

(http://iopscience.iop.org/0953-8984/19/14/145214)

IOP PUBLISHING JOURNAL OF PHYSICS: CONDENSED MATTER

J. Phys.: Condens. Matter **19** (2007) 145214 (9pp) doi:10.1088/0953-8984/19/14/145214

Study of ferromagnetic–spin glass threshold in $R_2Mo_2O_7$ by high-pressure neutron diffraction and μSR

A Apetrei[1], I Mirebeau[1], I Goncharenko[1], D Andreica[2,3] and P Bonville[4]

[1] Laboratoire Léon Brillouin, CEA-CNRS, CE-Saclay, 91191 Gif-sur-Yvette, France
[2] Laboratory for Muon-Spin Spectroscopy, Paul Scherrer Institut, 5232 Villigen-PSI, Switzerland
[3] Babes-Bolyai University, Faculty of Physics, 400084 Cluj-Napoca, Romania
[4] Service de Physique de l'Etat Condensé, CEA-CNRS, CE-Saclay, 91191 Gif-Sur-Yvette, France

E-mail: mirebea@llb.saclay.cea.fr

Received 12 December 2006
Published 23 March 2007
Online at stacks.iop.org/JPhysCM/19/145214

Abstract

We present a comparative study of $(Tb_{0.8}La_{0.2})_2Mo_2O_7$ and $Gd_2Mo_2O_7$ situated at the verge of a Mott transition from ferromagnetic metal to insulating spin glass, which can be tuned by the rare-earth ionic radius. We probe the spin correlations and fluctuations versus temperature and pressure thanks to neutron scattering and μSR. The ambient pressure state of ferromagnetic character shows striking differences between the two compounds, both in the static and dynamic properties, showing the influence of the Tb crystal field anisotropy. Under pressure, both compounds transform into a spin glass state. We also studied the chemically ordered spin glass $Tb_2Mo_2O_7$ with pressure and temperature. We observe mesoscopic ferromagnetic correlations between Tb moments, together with short-range correlations. All persist down to very low temperature (40 mK), showing that the spin glass order corresponds to the magnetic ground state. Under pressure, the lengthscale of the mesoscopic correlations is strongly reduced, whereas the short-range correlations are unchanged.

1. Introduction

$R_2T_2O_7$ pyrochlores, where R^{3+} is a rare-earth ion and T^{4+} is a transition-metal ion, form a large family of oxides with many unusual magnetic and conduction properties. The geometrical frustration of the pyrochlore lattice, which can exist in both R and T sublattices, yields the possibility of exotic magnetic states, such as spin liquids, spin ices, spin glasses with chemical order, as well as complex ordered magnetic structures. On the other hand, the strong intra-site Coulomb interaction between the electrons of the transition metal offers the possibility of inducing many anomalous conduction properties. Generally speaking, the trends are as follows. 3d transition-metal pyrochlores (like $R_2Ti_2O_7$) are insulating due to the strong

electron correlations and small electron transfer along O–T–O bonds. 4d transition-metal pyrochlores show an intermediate behaviour. They may be insulating ($R_2Sn_2O_7$), metallic ($R_2Mn_2O_7$ or $R_2Bi_2O_7$), or display an insulating–metal transition ($R_2Mo_2O_7$). 5d transition-metal pyrochlores are generally metallic, since the 5d orbitals are more extended than the 3d or the 4d orbitals, and hybridize more strongly with the oxygen p states. For some 5d ions, the influence of electrons correlations remains important, for example in $Cd_2Os_2O_7$ and $Cd_2Re_2O_7$, which behave as semi-metals with a Fermi level lying in a pseudogap [1] and show spectacular resistivity anomalies.

Within the pyrochlores, the 4d transition-metal $R_2Mo_2O_7$ are especially suitable for studying the interplay between magnetic and conduction properties. The Mo^{4+} 4d t_{2g} orbitals, situated nearby the Fermi level and well separated from the other bands [2, 3], play a dominant role in the band structure and the magnetic properties. As a direct probe of the influence of the Mo molecular field, the magnetic transition temperatures in $R_2Mo_2O_7$ are in the range 25–100 K, well above the transition temperatures of $R_2Sn_2O_7$ with non-magnetic Sn, which are around 1–2 K. Interestingly, the Mo magnetism can be tuned by the R ionic radius [4, 5]. Compounds with small ionic radius (R = Y, Tb) behave as insulating spin glasses with chemical order [6–8]. Compounds with large ionic radius (Sm, Nd) behave as ferromagnetic metals. $Nd_2Mo_2O_7$ was intensively studied, due to its giant abnormal Hall effect [9]. Although the exact mechanism is still debated [3, 10], the Nd crystal field anisotropy leading to spin ice frustration seems to play a key role. The chirality mechanism invoked recalls that proposed for metallic spin glasses [11–13].

Band structure calculations [3] and detailed investigations of many substituted $(RR')_2Mo_2O_7$ compounds show that the ferromagnetic–spin glass transition observed versus ionic radius in $R_2Mo_2O_7$ comes from a change in the sign of the Mo–Mo interactions. Ferromagnetic interactions in the metallic side become antiferromagnetic and thus geometrically frustrated on the insulating side of the phase diagram. The origin of this effect is the aperture of a Mott–Hubbard gap in the t_{2g} band due to intra-site electron correlations. The trigonal distortion of the Mo oxygen environment splits the t_{2g} band into a_{1g} and e'_g sub-bands. As the lattice constant decreases, the increasing Coulomb energy localizes the itinerant e'_g electrons, ferromagnetically coupled by a double exchange mechanism. Their contribution to the magnetic exchange interaction decreases at the expense of the a_{1g} ones, which interact antiferromagnetically by a superexchange mechanism mediated by oxygen 2p orbitals. The band structure calculation therefore closely correlates the dominant antiferromagnet (AF) interaction to the insulating character. Coming back to the real systems, some questions arise. Do the ferro-spin glass and insulating–metal transitions always coincide? What is the role of the rare-earth magnetism? How is an external pressure compared with the chemical pressure induced by the rare-earth ion? One should also understand how the ferromagnetic order transforms into the spin glass order. What is the evolution of the spin correlations and fluctuations? Do the spin glass (SG) and ferromagnet (F) orders coexist in some region of the phase diagram?

To find the answers to these questions, we studied two compounds in the ferromagnetic region close to the F–SG threshold. We used neutron diffraction, μSR and x-ray synchrotron radiation, at ambient and under applied pressure. In $(Tb_{0.8}La_{0.2})_2Mo_2O_7$, we have induced ferromagnetism by expanding the lattice through Tb/La substitution [14]. $Gd_2Mo_2O_7$ has been widely studied using various techniques [15–18], but never by neutrons due to its huge absorption, nor by muons. Our detailed results on $Gd_2Mo_2O_7$ are reported in [19]. In contrast with Tb, the Gd ionic moment has no orbital component. Here we present a comparative study of the two compounds, as well as new results on $Tb_2Mo_2O_7$ spin glass, studied by neutrons down to 40 mK and under applied pressure.

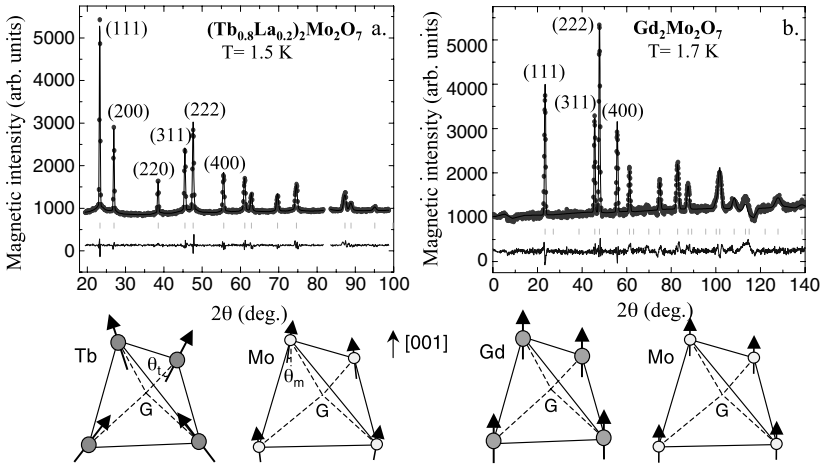

Figure 1. Magnetic neutron intensity versus the scattering angle 2θ: (a) TbLa sample at $T = 1.5$ K, ambient pressure and neutron incident wavelength $\lambda = 2.426$ Å. (b) Gd sample at $T = 1.7$ K, ambient pressure and $\lambda = 2.419$ Å. A pattern in the paramagnetic range (70 and 90 K for TbLa and Gd samples, respectively) was subtracted. Solid lines show the best refinement and the difference spectrum. At the bottom are the corresponding spin arrangements of Tb, Gd and Mo tetrahedra.

2. Experimental details

Ambient pressure powder neutron diffraction measurements on $(Tb_{1-x}La_x)_2Mo_2O_7$ ($x = 0$ and 0.2) were performed on G61 and G41 diffractometers of the Laboratoire Léon Brillouin (LLB) down to 1.4 K and down to 40 mK on the D1B diffractometer of the Institute Laüe Langevin (ILL). As for $Gd_2Mo_2O_7$, we used isotopically enriched ^{160}Gd and the high-flux diffractometers D20 and D2B of the ILL. High-pressure neutron diffraction patterns were recorded on the G61 (LLB) in the high-pressure version [20]. μSR measurements were performed at the Swiss Muon Source at the Paul Scherrer Institute (PSI) on GPS (ambient pressure) and GPD (under pressure). The equation of state was determined by x-ray diffraction under pressure using the synchrotron radiation at the ID27 beam line of the European Synchrotron Radiation Facility (ESRF).

3. Comparison of two compounds: $(Tb_{0.8}La_{0.2})_2Mo_2O_7$ and $Gd_2Mo_2O_7$

Both compounds are situated in the ferromagnetic region of the phase diagram ($a > a_c$) with lattice constants of $a = 10.3787(8)$ Å and 10.3481(2) Å for TbLa and Gd samples, respectively. From [4], we get $a_c \sim 10.33$ Å. The Curie temperatures T_C, deduced from susceptibility data, are 58 K (TbLa sample) and 70 K (Gd sample).

To compare their magnetic ground states, we consider the magnetic diffraction patterns well below T_C (figure 1), at 1.5 and 1.7 K respectively. The magnetic Bragg peaks belong to the face-centred cubic lattice, showing that in both cases the magnetic structure is derived from the chemical structure of the $Fd\bar{3}m$ symmetry by a propagation vector $\mathbf{k} = 0$. Therefore one R/Mo tetrahedron describes the magnetic structure. As a striking feature, for the TbLa sample we observe two magnetic peaks (200) and (220), which cannot be observed for the Gd sample. These peaks are forbidden by the chemical structure of the pyrochlore lattice. Their observation in the TbLa sample means that the spin arrangement is non-collinear.

By refining the magnetic structures, we see that for the TbLa sample the Tb moments are close to the local ⟨111⟩ anisotropy axis (with an angle $\theta_t \sim 11.5°$). They are oriented in the 'two in, two out' configuration of the local spin ice structure [21], which yields F components along [001]. The Mo moments align close to a [001] axis, with a slight tilting angle $\theta_m \sim 7°$. In the Gd sample, the magnetic structure corresponds to a collinear ferromagnet. For both compounds, the R and Mo moments are ferromagnetically coupled, in contrast with $Nd_2Mo_2O_7$. All ordered moments are strongly reduced (by about 50% for the Tb, 30% for the Gd ions, and up to 70% for Mo) with respect to the free ion values (9 μ_B for Tb, 7 μ_B for Gd and 2 μ_B for Mo). For Tb this reduction is partly explained by a change of Tb environment when diluted with non-magnetic La ions, but it should also come from crystal field effects. For Gd and Mo, it may arise either from quantum fluctuations due to the proximity of the threshold, or from the frustration of the orbital component of the Mo moment [3].

In both cases the ground state is determined by the Mo–Mo F exchange interaction. The difference in spin arrangements emphasizes the role of the strong uniaxial anisotropy of the Tb^{3+} ion compared to the Gd^{3+} ion, which is isotropic. The anisotropy of Tb^{3+} brings spin ice frustration into the ferromagnetic state.

With increasing temperature, the ordered spin ice structure found for the TbLa sample at low temperature is kept up to the Curie point, with a decrease in the canting angles. On the contrary, in the Gd sample, the ferromagnetic model does not fully account for the T dependence of the Bragg peaks, but no better magnetic structure could be found.

Looking at the magnetic fluctuations using μSR, we observed important new differences between the two compounds. The fit of the μSR depolarization function $P_Z(t)$ measured below T_C involves four parameters [14, 19]. The first two, which govern the long-time relaxation, are the longitudinal relaxation rate λ_Z and its exponent β. They reflect the spin dynamics. The others, which account for the strong depolarization at early times and the wiggles respectively, are the transverse relaxation rate, λ_T, and the average local field, $\langle B_{loc} \rangle$, at the muon site. Considering that $\lambda_T \gg \lambda_Z$, we associate λ_T with the distribution of *static* local fields.

As shown in figure 2 (right), the temperature dependence of the 'static' terms is similar in the two compounds and shows no anomaly with temperature. $\langle B_{loc} \rangle$ and λ_T scale with each other and with the R ordered moment (Tb or Gd) determined by neutron diffraction. It shows that the local magnetic field on the muon site is dominated by the R moment, much more than that of Mo.

Striking differences appear in the dynamic terms (figure 2, left). The T dependence of λ_Z shows a critical peak at T_C due to the onset of magnetic order. In a standard ferromagnet, the contribution of spin waves should yield a decrease of λ_Z below T_C, down to zero at $T = 0$. Here two types of abnormal behaviours are observed. In TbLa sample, λ_Z shows a broad maximum at $T^\star \sim 25$ K. It suggests a second transition of dynamical nature since there is no anomaly in the static terms. In Gd sample, the broad maximum is either strongly reduced or completely suppressed. λ_Z remains almost constant within the accuracy of the measurements, and close to its value above T_C down to 6 K. Finally, in TbLa sample, the β exponent (not shown) is strongly temperature dependent whereas it remains constant and equal to 1 in Gd sample.

Under pressure, the ferromagnetic order in both compounds is gradually destroyed [14, 17, 19]. We can follow this evolution both by μSR and by neutrons. T_C decreases under pressure and the two transitions observed for TbLa sample seem to merge. The Bragg peak intensity decreases under pressure and short range correlations arise. Figure 3 shows the spin correlations in TbLa at 3.7 GPa ($a \sim 10.298$ Å) and Gd sample at 2.7 GPa ($a \sim 10.289$ Å). The short range order modulations are akin to that in $Tb_2Mo_2O_7$ at ambient pressure (see below).

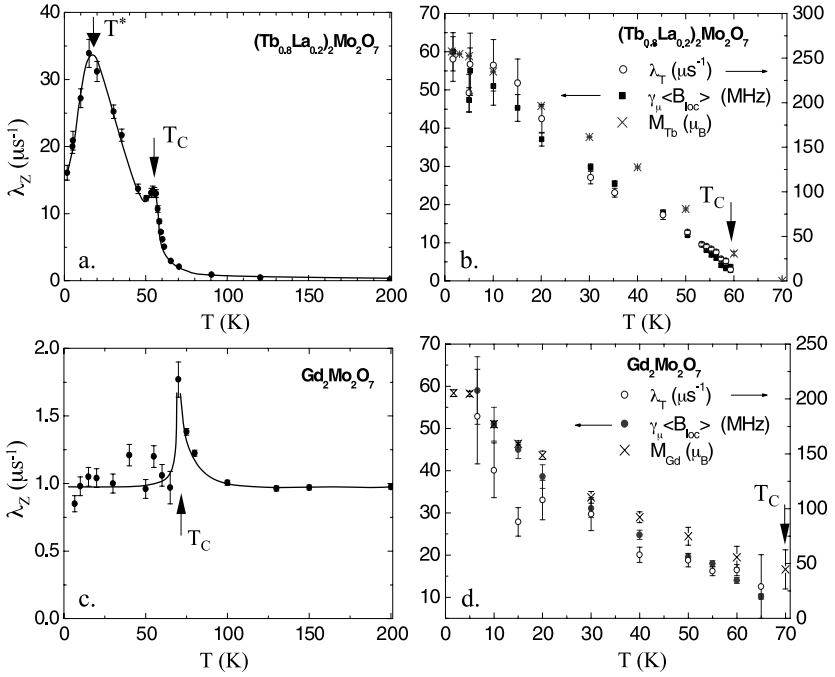

Figure 2. μSR ambient pressure results: TbLa sample, temperature dependence of (a) λ_Z; (b) λ_T, $\langle B_{loc}\rangle$ (with γ_μ being the muon gyromagnetic ratio) and ordered magnetic moment M_{Tb} (scaled); Gd sample, temperature dependence of (c) λ_Z; (d) λ_T, $\langle B_{loc}\rangle$, M_{Gd} (scaled). Lines are guides to the eye.

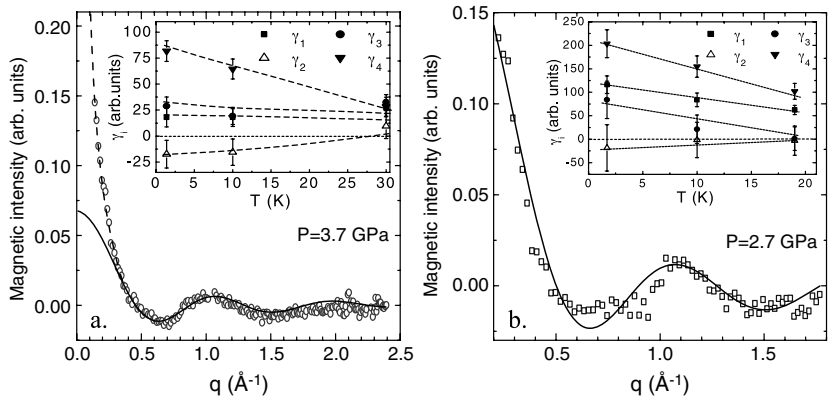

Figure 3. Magnetic intensity versus the scattering vector $q = 4\pi \sin\theta/\lambda$, with $\lambda = 4.741$ Å. A pattern in the paramagnetic region (100 K) was subtracted. (a) TbLa sample, at $T = 1.4$ K and $P = 3.7$ GPa. (b) Gd sample, at $T = 1.5$ K and $P = 2.7$ GPa. Lines are fits as described in the text. In the inset are the temperature dependence of the correlations coefficients. Dashed lines are guides to the eye.

The magnetic correlations were analysed with the short-range order (SRO) model described in [6]. This allows the determination of spin correlation parameters γ up to the fourth coordination cell, as seen in the two insets. For both samples, $\gamma_{1,3,4} > 0$ and $\gamma_2 < 0$. Considering the relative amplitude of the magnetic moments, it means that the R–R correlations

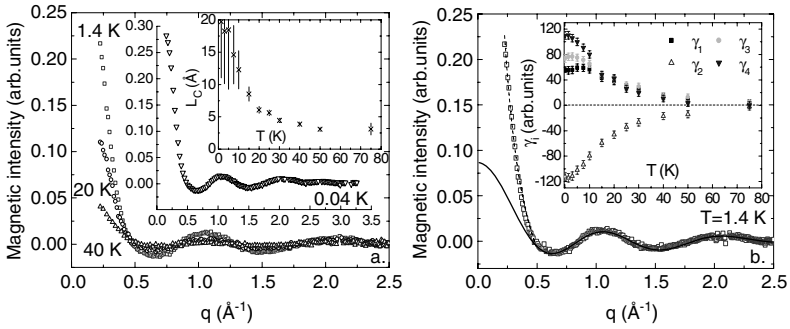

Figure 4. (a) Magnetic intensity in $Tb_2Mo_2O_7$: $T = 1.4, 20, 40$ K ($\lambda = 4.741$ Å) and $T = 0.04$ K ($\lambda = 2.52$ Å) in the first inset. A pattern at 100 K was subtracted. Second inset: temperature dependence of correlation length L_C. (b) Fit of 1.4 K spectrum with the SRO model (bottom line) including the longer-range F correlations (upper dashed line) with the corresponding correlation parameters in the inset.

(which control the $\gamma_{1,3,4}$ terms) are F, while the R–Mo correlations (γ_2) become AF under pressure.

The R–R ferromagnetic correlations are shown by intense scattering at low angles ($q < 0.5$ Å^{-1}). In the Gd sample at 2.7 GPa, they can be fitted by the SRO model (figure 3(b)), showing that they extend to four neighbours only (∼7 Å). In the TbLa sample at 3.7 GPa, the SRO model cannot account for them (figure 3(a)), since they extend to a longer length scale (about 18 Å).

4. $Tb_2Mo_2O_7$

We first analyse the ambient pressure magnetic correlations in $Tb_2Mo_2O_7$ ($a \sim 10.31$ Å), which is a well-known spin glass without chemical disorder and with a spin glass transition at $T_F \sim 25$ K. Besides the diffuse magnetic scattering observed for $q > 0.5$ Å^{-1}, denoting SRO as reported in [6, 7], we also observe intense small-angle neutron scattering (SANS) below this q value. This corresponds to the onset of F correlations with a mesoscopic length scale. The temperature evolution of magnetic correlations (figure 4(a)) clearly shows the increase in F correlations with decreasing temperature. By performing neutron diffraction measurements down to 40 mK, we show that the magnetic correlations saturate below 1.4 K. Their observation down to 40 mK (0.002 T_F) proves that the spin glass state is indeed the ground state of this compound.

Figure 4(b) shows the fits of $Tb_2Mo_2O_7$ magnetic spectra at 1.4 K. For $q > 0.5$ Å^{-1} we used the same model as in [6] (see figure 4(b) bottom line). The correlation parameters are plotted in the inset. As for the TbLa and Gd samples under pressure, we get $\gamma_{1,3,4} > 0$ and $\gamma_2 < 0$, which show F R–R and AF R–Mo correlations. As for TbLa, the SRO model cannot describe the SANS signal, which was fitted by adding a Lorentzian function (upper dashed line). The correlation length of the Lorentzian ($L_C \sim 20$ Å at 1.4 K) decreases with increasing temperature (second inset figure 4(a)).

Figure 5, which compares magnetic spectra at $P = 0$ and 5.3 GPa ($a \sim 10.201$ Å), clearly shows that the SANS signal and hence the corresponding F R–R mesoscopic correlations decrease with increasing pressure. The correlation length decreases under pressure and the SRO model now yields a good fit in the whole q interval, as for the Gd sample under pressure.

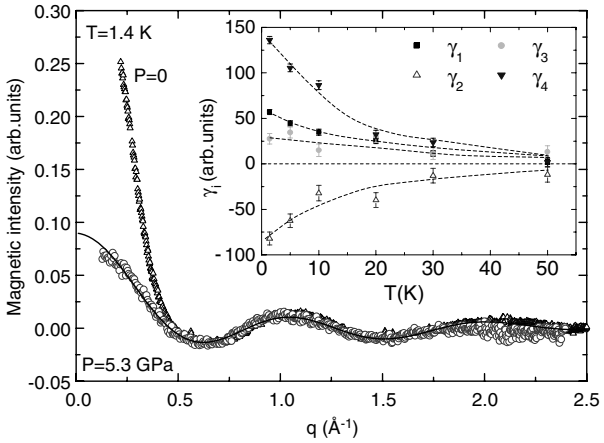

Figure 5. Magnetic intensity in $Tb_2Mo_2O_7$ at 1.4 K, $\lambda = 4.741$ Å: ambient (△) and applied pressure (○). A pattern at 100 K was subtracted. The fit of the $P = 5.3$ GPa data is made using the SRO model. The temperature dependence of correlation coefficients is shown in the inset, with dashed lines as guides to the eye.

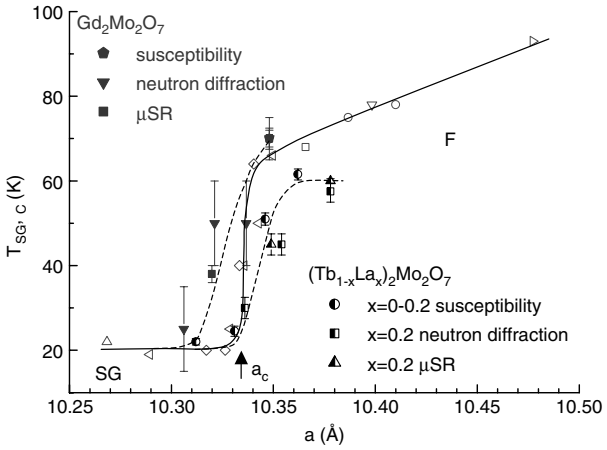

Figure 6. Phase diagram in the threshold region: general curve from [4, 5, 8] (open symbols), $(Tb_{1-x}La_x)_2Mo_2O_7$ (half filled symbols) and GdMo (filled symbols). Lines are guides to the eye.

The modulations above 0.5 $Å^{-1}$ are almost unchanged by pressure. The correlation parameters keep the same sign as at ambient pressure (inset of figure 5), yielding F R–R and AF R–Mo correlations, respectively. Their values at ambient and under pressure are similar in the limit of the error bars.

5. Discussion

5.1. The threshold region

An experimental phase diagram of the $R_2Mo_2O_7$ transition temperature against the cell parameter is shown in figure 6. At ambient pressure, our starting points for the Gd and TbLa samples slightly deviate from the general curve drawn according to [4, 5]. This could be due

to sample preparation. The Gd sample is very sensitive to it, with a T_C variation between 40 and 70 K reported in the literature. As for the TbLa sample, it may be due to La dilution close to the solubility limit. Besides these initial offsets, our results show the same behaviour under applied pressure as the general curve obtained under chemical pressure. They show how the LRO transforms in SRO passing through a region where the two signals coexist, providing a microscopic description of the F–SG threshold region (for details, see [14, 19]).

5.2. Dynamical transition in the ferromagnetic regime

In the TbLa sample, where the uniaxial Tb anisotropy yields a non-collinear ground state, we have observed a second transition using μSR, akin to that previously observed in re-entrant spin glasses [22, 23]. Recent μSR measurements [24] show that it also exists in $Sm_2Mo_2O_7$, where the magnetic structure is unknown but the Sm anisotropy is supposed to be planar. The temperature variation of the β exponent in the TbLa sample and in $Sm_2Mo_2O_7$ suggests a large distribution of relaxation rates, as in spin glasses [25]. In contrast, in $Gd_2Mo_2O_7$, where the Gd moment is isotropic and the ground state is collinear, there seems to be no second transition (or at least it is strongly suppressed) and we get $\beta = 1$. It is therefore tempting to connect the second transition with magnetic frustration on the R site induced by R anisotropy. In re-entrant spin glasses, the second transition was attributed to the freezing of transverse spin components with a mesoscopic length scale, which agrees with mean field theory [26]. In the TbLa sample, we have observed, below the Bragg peaks of the spin ice ordered structure, a magnetic background coming from short-range ordered moments, having the same type of correlations as the LRO. These moments start to correlate at around 40 K, namely between T_C and $T^\star$. It could be assumed that they remain paramagnetic at T_C, and start to correlate and freeze when T decreases further. An energy analysis of the SRO by inelastic neutron scattering should allow us to check the occurrence of this freezing on the neutron time scale. The neutron time scale ($\tau \sim 10^{-11}$ s) is much shorter than the muon time scale, so the freezing transition should occur above the $T^\star$ value probed by muons.

5.3. Spin glass state under pressure

As has already been stated, the F–SG transition is controlled by the Mo–Mo interactions. At ambient pressure, the magnetic interactions are ferromagnetic in both the TbLa and Gd samples. Their magnetic structures show that all correlations (Mo–Mo, R–Mo and R–R) are ferromagnetic. Under pressure the distances Mo–Mo are reduced and hence the balance between the double exchange F and superexchange AF interactions is changed: the AF Mo–Mo interactions are favoured. In both systems the ferromagnetic phase transforms into a spin glass state characterized by short-range correlations similar to that observed for $Tb_2Mo_2O_7$. Our observations provide a microscopic description of the pressure-induced spin glass state recently inferred from magnetic measurements [17, 27]. Besides the change in the Mo–Mo interactions which induce the spin glass frustration, the SRO model shows that, under pressure, the R–Mo correlations change to AF. The R–R correlations remain F, but they are strongly reduced under pressure, as shown by our study of $Tb_2Mo_2O_7$. What is the origin of the R–Mo and R–R correlations and why do they change with pressure? Our present study of the three compounds shows that these correlations do not arise from the rare-earth anisotropy and persist under La doping. Previous simulations of the diffuse scattering in $Tb_2Mo_2O_7$ [6, 28] show that correlations are not very sensitive to Mo–Mo interaction due to the small Mo moment. The R–Mo and R–R correlations could arise from R–Mo interaction, which involves the Mo t_{2g} band together with the 4f levels of the R ion. This interaction may be sensitive to pressure, though less than the Mo–Mo interaction.

In conclusion, neutron diffraction and μSR combined with high-pressure techniques are a useful tool to study the ferro-spin glass threshold in $R_2Mo_2O_7$ pyrochlores. The changes in the spin correlations can be studied in detail when encompassing the threshold, as well as the anomalous fluctuations at the verge of the Mott transition.

Acknowledgments

We thank O Isnard, E Suard and G André for their help in the neutron measurements on D1B, D20 and G41, respectively. We also thank A Amato and U Zimmermann for the μSR measurements on GPS and GPD and W Crichton for the x-ray measurements on ID27. We thank A Forget and D Colson for the sample preparation and J P Sanchez for providing the ^{160}Gd isotope and for useful discussions.

References

[1] Singh D H, Blaha P, Schwartz K and Sofo J O 2002 *Phys. Rev.* B **65** 155109
[2] Kang J S *et al* 2002 *Phys. Rev.* B **65** 224422
[3] Solovyev I V 2003 *Phys. Rev.* B **67** 174406
[4] Katsufuji T, Hwang H Y and Cheong S-W 2000 *Phys. Rev. Lett.* **84** 1998
[5] Moritomo Y *et al* 2001 *Phys. Rev.* B **63** 144425
[6] Greedan J E *et al* 1991 *Phys. Rev.* B **43** 5682
[7] Gaulin B D *et al* 1992 *Phys. Rev. Lett.* **69** 3244
[8] Gingras M J P *et al* 1997 *Phys. Rev. Lett.* **78** 947
[9] Taguchi Y *et al* 2001 *Science* **291** 2573
[10] Yasui Y *et al* 2006 *Preprint* cond-mat/0603045
[11] Kawamura H 2003 *Phys. Rev. Lett.* **90** 47202
[12] Pureur P *et al* 2004 *Europhys. Lett.* **67** 123
[13] Taniguchi T *et al* 2004 *Phys. Rev. Lett.* **93** 246605
[14] Apetrei A, Mirebeau I, Goncharenko I, Andreica D and Bonville P 2006 *Phys. Rev. Lett.* **97** 206401
[15] Hodges J A *et al* 2003 *Eur. Phys. J.* **33** 173
[16] Kézsmárki I *et al* 2004 *Phys. Rev. Lett.* **93** 266401
[17] Park J G *et al* 2003 *Physica* B **328** 90
[18] Hanasaki N *et al* 2006 *Phys. Rev. Lett.* **96** 116403
[19] Mirebeau I *et al* 2006 *Phys. Rev.* B **74** 174414
(Mirebeau I *et al* 2006 *Preprint* cond-mat/0606420)
[20] Goncharenko I 2004 *High Pressure Res.* **24** 193
[21] Bramwell S T and Gingras M J P 2001 *Science* **294** 1495
[22] Mirebeau I *et al* 1997 *Hyper. Interface* **104** 343
[23] Ryan D H *et al* 2000 *Phys. Rev.* B **61** 6816
Ryan D H *et al* 2004 *J. Phys.: Condens. Matter* **16** S4619
[24] Jo Y *et al* 2005 *J. Korean Phys. Soc.* **47** 123
[25] Campbell I A *et al* 1994 *Phys. Rev. Lett.* **72** 1291
[26] Gabay M and Toulouse G 1981 *Phys. Rev. Lett.* **47** 201
[27] Miyoshi K, Takamatsu Y and Takeuchi J 2006 *J. Phys. Soc. Japan* **75** 065001
[28] Reimers J N 1992 *Phys. Rev.* B **46** 193